Spectral signatures of climate change in the Earth's infrared spectrum between 1970 and 2006

Claudine Chen [1], John Harries [1], Helen Brindley [1], Mark Ringer [2]

[1] Department of Physics, Imperial College London
[2] Hadley Centre, UK Met Office

Abstract

Previously published work using satellite observations of the clear sky infrared emitted radiation by the Earth in 1970, 1997 and in 2003 showed the appearance of changes in the outgoing spectrum, which agreed with those expected from known changes in the concentrations of well-mixed greenhouse gases over this period. Thus, the greenhouse forcing of the Earth has been observed to change in response to these concentration changes. In the present work, this analysis is being extended to 2006 using the TES instrument on the AURA spacecraft. Additionally, simulated spectra have been calculated using LBLRTM with inputs from the HadGEM1 coupled model and compared to the observed satellite spectra.

INTRODUCTION

This paper extends the previous work done by this group [*Griggs and Harries*, 2007; *Harries, et al.*, 2001] to include data from 2006 from the Tropospheric Emission Spectrometer (TES) on the AURA satellite. Prior studies have compared data from 1970 (with the Infrared Interferometer Spectrometer, IRIS) to 1997 (with the Interferometric Monitor of Greenhouse gases, IMG) and 2003 (with the Atmospheric Infrared Sounder, AIRS). Changes were detected in the spectra that were attributed to known changes in greenhouse gas concentrations.

OBSERVATIONS AND DATA

The previous work compared consecutive data from April, May and June over the central Pacific (180 – 130°W, 10°S – 10°N). The current work comparing data from TES from 2006 to IRIS data from 1970 uses the same spatial and temporal limits for consistency.

IRIS, flown on Nimbus 4, is a Fourier transform spectrometer (FTS) with apodized spectral resolution of 2.8 cm^{-1} and a nadir field of view that corresponds to a ground footprint of 95 km in diameter. The instrument was launched in April 1970 and recorded data until January 1971 [*Hanel and Conrath*, 1970; *Hanel, et al.*, 1972]. IRIS recorded spectra between 400 and 1600 cm^{-1} but wavenumbers above about 1400 cm^{-1} suffer from high noise. TES is an FTS instrument on the AURA satellite launched in 2004 [*Beer, et al.*, 2001]. Global surveys are collected every 2 days, and take roughly 24 hours to collect. These global surveys collect four bands of spectra discontinuously over the wavenumber range of 650 – 2260 cm^{-1}; we use three bands over 650 – 1350 cm^{-1} for this analysis. The data over the 16 pixel detector is averaged, corresponding to a footprint of 5.3x8.5 km. The two satellite instruments have different spectral properties that need careful treatment before direct comparison can be performed.

TES data, acquired at a higher spectral resolution than IRIS at 0.1 cm^{-1}, was smoothed to the IRIS spectral resolution by convolution with the IRIS instrument line function, a Hamming function with a width of 2.8 cm^{-1}. The difference in the field of view between the two instruments must also be considered. The effect of a finite field of view is to broaden spectral features and shift them to lower wavenumbers, since off-axis rays travel a longer path through the interferometer than on-axis rays. [*Thorne*, 1988] This effect is compensated for using a known theoretical relation. Matching of spectral

features is further fine tuned by increasing the spectral sampling of both spectra and matching the minima of known absorption features. The increase in the spectral sampling is done by zero-fill interpolation [*Forman*, 1966], in which the interferogram of the spectrum is increased in size and padded with zeroes at the high frequency end before being transformed back to the spectral domain.

To reduce the variability seen in the spectrum, cloud-free spectra are used. A two step process was used to identify clouds in the spectra [*Harries, et al.*, 2001]. The first step is to filter out thick clouds by comparing the brightness temperature at 1127.7 cm^{-1} (most transparent part of spectral range) with the skin temperature from the NCEP reanalysis. Differences greater than 6 K between the NCEP skin temperature and observed brightness temperature were flagged as cloudy [*Haskins, et al.*, 1997]. The second step removes spectra with residual contamination from ice clouds. This is done by exploiting the difference in absorption coefficient in ice and water between the 8 um and 11 um bands. [*Ackerman, et al.*, 1990]

MODELLING OF SPECTRA

Comparison of observed spectra to modelled spectra is a stringent test of our ability to model processes in the atmosphere that affect outgoing longwave radiation. We study the consistency of our observed spectra with modelled spectra using output from the UK Met Office HadGEM1 coupled model [*Johns, et al.*, 2006; *Martin, et al.*, 2006], with historic and realistic (IPCC) projections of greenhouse gas amounts. [*Stott, et al.*, 2006]

Spectra were simulated using the line-by-line radiative transfer model (LBLRTM) [*Clough, et al.*, 2005], version 10.3, at a spectral resolution of 0.1 cm^{-1}. LBLRTM was run with user-defined profiles constructed using monthly mean HadGEM1 output fields of specific humidity, temperature, and sea surface temperature from the global circulation model for April, May, and June of 1970 to simulate IRIS spectra. The process was then repeated for profiles from 2006 to simulate TES spectra. In each case, the concentrations of CO_2, CH_4, O_3, N_2O, CFC-11, CFC-12, CFC-113, and HCFC-22 used within HadGEM1 at the relevant times were also used to provide input to the radiative transfer model calculations. In both cases the profiles above the altitudes provided by the model were padded with standard tropical atmosphere values [*Anderson, et al.*, 1986]. The spectroscopic data used within the RT code was compiled by AER version 1.0, based on HITRAN 2000 with updates to some molecules [*Clough, et al.*, 2005]. The spectral resolution of each simulated spectrum was then reduced to match the IRIS observational value of 2.8 cm^{-1} using the appropriate Hamming window.

As intimated above, to simulate the average spectrum, we calculate the spectrum of the average atmospheric state rather than calculate the average of many simulated spectra, one for each model grid box, which is computationally expensive. Previous analysis has found that the use of the averaged profiles to be within 0.2 K of the more computationally intensive method [*Griggs and Harries*, 2007].

RESULTS

In Figure 1, the IRIS spectrum, averaged over cloud-cleared data in April, May, and June of 1970 in the central Pacific, is compared to the simulated spectrum calculated by LBLRTM from the average state of the HadGEM1 model for the same temporal and spatial limits as the observed data. The observed – modelled difference spectrum is within 1 K in the window region except for some small water features. Factors that influence the spectral response of the window region are ice and water clouds, surface temperature, and low level water vapour. The asymmetry across the 9.6 µm ozone band of the difference spectrum suggests contribution from ice or water clouds or low level water vapour. The signal of the modelled methane at 1304 cm^{-1} is deeper than the observed signal by almost 5 K, suggesting that either the mid to upper tropospheric temperature in the model is too low or that the amount of methane in the simulations is too high. The 9.6 um ozone band has not been analyzed in any of these cases, since it is known to be highly variable and is outside the scope of this paper.

In Figure 2, the comparison of the observed TES data vs. modelled 2006 case is shown. Similar to the IRIS case, the TES spectrum is averaged over cloud-cleared data in April, May, and June of 2006 in the central Pacific, and the modelled data is calculated by LBLRTM from the average state of the HadGEM1 model for the same temporal and spatial limits as the observed data. The model simulates the methane signal better in this case, with the methane signal roughly 1-2 K in difference. The observed – modelled difference spectrum is similarly to the IRIS case within 1 K in the window region except for some small water features. Again, the asymmetry across the 9.6 µm ozone band of the difference spectrum suggests contribution from ice or water clouds or low level water vapour. However, TES has a smaller footprint than IRIS, and the amount of cloud contamination is expected to be smaller for TES. Since TES and IRIS have similar signatures in the window region, we assert that cloud contamination is not a predominant source of this signal.

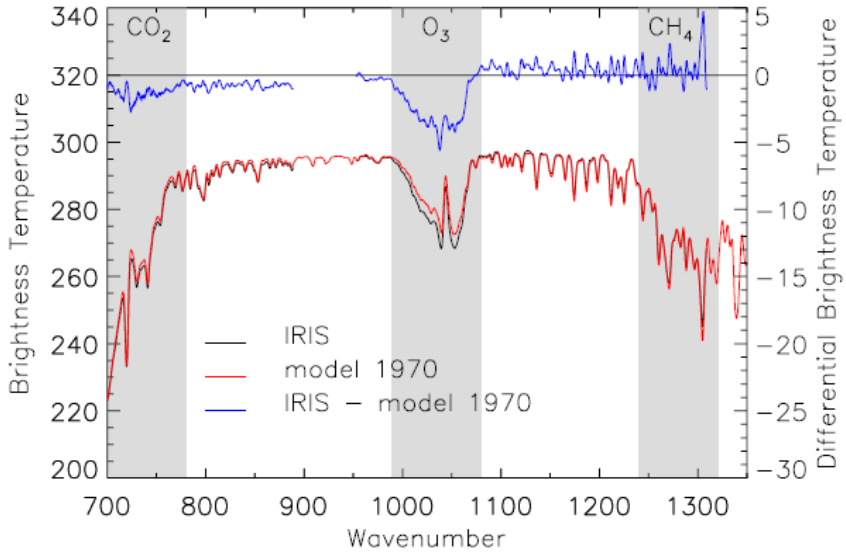

Figure 1. Averaged IRIS spectrum (black line) in brightness temperature and averaged simulated spectrum (red line) with the scale on the left axis. The observed – modeled spectrum (green line) is plotted against the right axis. Relevant absorption bands are shaded in grey and labeled with the associated species.

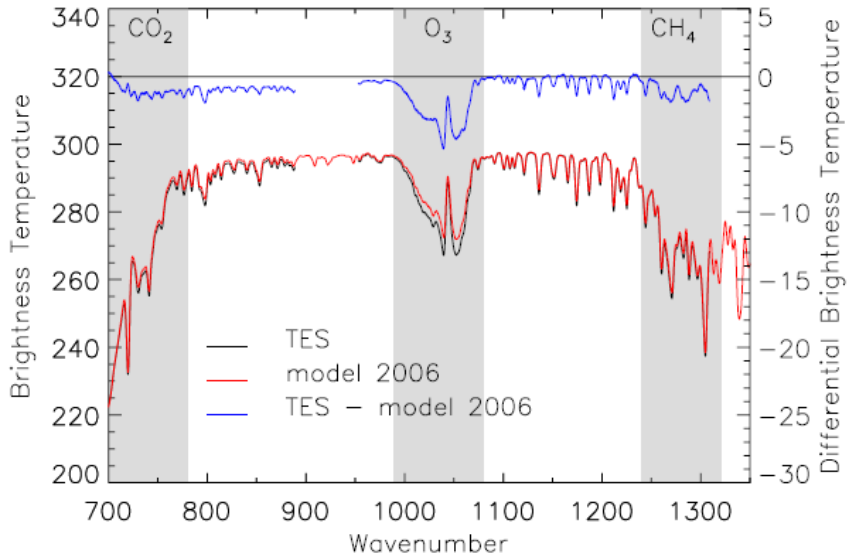

Figure 2. Averaged TES spectrum (black line) in brightness temperature and averaged simulated spectrum (red line) with the scale on the left axis. The observed – modeled spectrum (green line) is plotted against the right axis. Relevant absorption bands are shaded in grey and labeled with the associated species.

The observed TES – IRIS and simulated 2006 – 1970 difference spectra are shown in Figure 3. The background offset in the lower wavenumber window discussed previously when comparing the observed and modelled brightness temperature spectra (Figure 1 and Figure 2) is not apparent when comparing the observed and modelled difference spectra. Instead the feature cancels out and the background is seen to match well over the wing of the 15 µm CO_2 band and in the window regions. This emphasizes the importance of looking at the raw spectra as well as the difference spectra. The modelled 2006 – 1970 difference in the methane signal is shallower than the observed case, which is due to the model calculating a deeper signal for 1970 than was observed.

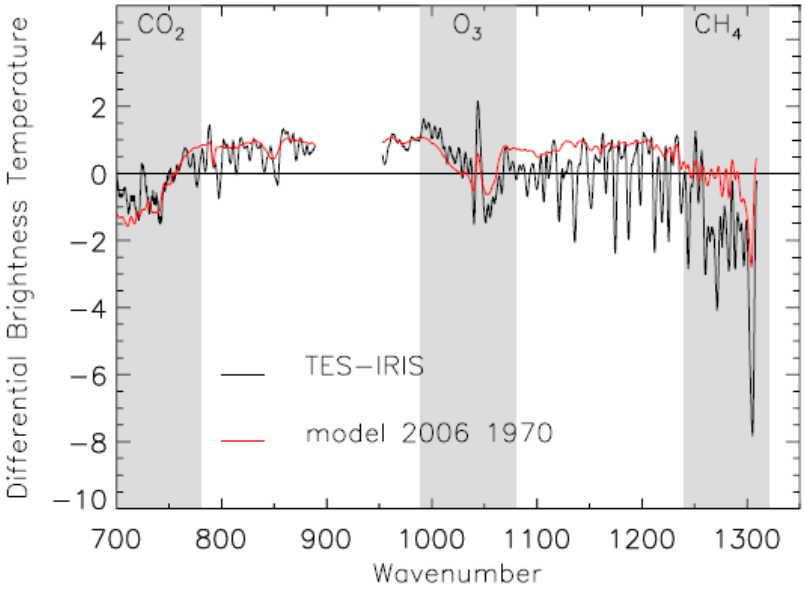

Figure 3. Observed difference spectrum (black line) between 2006 and 1970 (TES – IRIS) and the simulated difference spectrum (red line) for the same time interval.

CONCLUSIONS

The TES data compare very well with the IRIS data, suggesting successful normalization of the different instrument characteristics. The TES and IRIS difference spectrum covers the time range of 1970 – 2006, a period of 36 years. Simulated spectra represent the state of the HadGEM1 coupled model for 1970 and 2006. Changing spectral signatures in CH_4, CO_2, and H_2O are observed, with the difference signal in the CO_2 matching well between observations and modelled spectra. The methane signal is deeper for the observed difference spectrum than the modelled difference spectrum, but this is likely due to incorrect methane concentrations or temperature profiles from 1970. In the future, we plan to extend the analysis to more spatial and temporal regions, other models, and to cloudy cases.

REFERENCES

Ackerman, S. A., et al. (1990), The 27-28 October 1986 Fire Ifo Cirrus Case-Study - Spectral Properties of Cirrus Clouds in the 8-12 Mu-M Window, *Monthly Weather Review*, *118*, 2377-2388.

Anderson, G. P., et al. (1986), AFGL Atmospheric Constituent Profiles (0.120km), *Environmental research papers*, *964*.

Beer, R., et al. (2001), Tropospheric emission spectrometer for the Earth Observing System's Aura Satellite, *Applied Optics*, *40*, 2356-2367.

Clough, S. A., et al. (2005), Atmospheric radiative transfer modeling: a summary of the AER codes, *Journal of Quantitative Spectroscopy & Radiative Transfer*, *91*, 233-244.

Forman, M. L. (1966), Fast Fourier-Transform Technique and its Application to fourier Spectroscopy, *Journal of the Optical Society of America*, *56*, 978.

Griggs, J. A., and J. E. Harries (2007), Comparison of spectrally resolved outgoing longwave radiation over the tropical Pacific between 1970 and 2003 using IRIS, IMG, and AIRS, *Journal of Climate*, *20*, 3982-4001.

Hanel, R. A., and B. J. Conrath (1970), Thermal Emission Spectra of Earth and Atmosphere from Nimbus-4 Michelson Interferometer Experiment, *Nature*, *228*, 143-&.

Hanel, R. A., et al. (1972), Nimbus 4 Infrared Spectroscopy Experiment .1. Calibrated Thermal Emission-Spectra, *Journal of Geophysical Research*, *77*, 2629-&.

Harries, J. E., et al. (2001), Increases in greenhouse forcing inferred from the outgoing longwave radiation spectra of the Earth in 1970 and 1997, *Nature*, *410*, 355-357.
Haskins, R. D., et al. (1997), A statistical method for testing a general circulation model with spectrally resolved satellite data, *Journal of Geophysical Research-Atmospheres*, *102*, 16563-16581.
Johns, T. C., et al. (2006), The new Hadley Centre Climate Model (HadGEM1): Evaluation of coupled simulations, *Journal of Climate*, *19*, 1327-1353.
Martin, G. M., et al. (2006), The physical properties of the atmosphere in the new Hadley Centre Global Environmental Model (HadGEM1). Part I: Model description and global climatology, *Journal of Climate*, *19*, 1274-1301.
Stott, P. A., et al. (2006), Transient climate simulations with the HadGEM1 climate model: Causes of past warming and future climate change, *Journal of Climate*, *19*, 2763-2782.
Thorne, A. (1988), *Spectrophysics*, Chapman and Hall.